AGU PUBLICATIONS

Geophysical Research Letters

RESEARCH LETTER
10.1002/2014GL060713

Key Points:
- There exist a local maximum and minimum in the E_a for shear heating
- Higher values of the initial temperature produce a larger local maximum in E_a
- The amount of shear heating increases with E_a in a nonlinear manner

Supporting Information:
- Readme
- Sections A1–A3 and Table S1

Correspondence to:
B.-D. So,
qudekf1@snu.ac.kr

Citation:
So, B.-D., and D. A. Yuen (2014), Stationary points in activation energy for heat dissipated with a power law temperature-dependent viscoelastoplastic rheology, *Geophys. Res. Lett.*, *41*, 4953–4960, doi:10.1002/2014GL060713.

Received 30 MAY 2014
Accepted 4 JUL 2014
Accepted article online 7 JUL 2014
Published online 25 JUL 2014

Stationary points in activation energy for heat dissipated with a power law temperature-dependent viscoelastoplastic rheology

B.-D. So[1] and D. A. Yuen[2,3,4]

[1]School of Earth and Environmental Sciences, Seoul National University, Seoul, South Korea, [2]Minnesota Supercomputing Institute, University of Minnesota, Twin Cities, Minneapolis, Minnesota, USA, [3]Department of Earth Sciences, University of Minnesota, Twin Cities, Minneapolis, Minnesota, USA, [4]School of Environment Studies, China University of Geosciences, Wuhan, China

Abstract We report that there exist a local maximum and minimum in the activation energy E_a describing mechanical heat dissipation of olivine for a given initial temperature and amount of deformation. The stationary point for the minimum dissipation is ~200 kJ/mol lower than that for the maximum. For larger activation energy than the stationary point for maximum dissipation, plastic deformation is sharply weakened and the temperature rise disappears altogether. Higher values of the initial temperature produce a larger local maximum for activation energy. The amount of heat dissipation increases with E_a in a nonlinear manner. Our results have direct ramifications on shear zone, which is governed by the amount of mechanical heat dissipation. We have observed them over a wide range of temperature and deformation boundary conditions. Our two-dimensional model study can provide valuable insight to enable greater predictive capability for the development of geodynamic shear zone in planetary-scale plate tectonics.

1. Introduction

The development of geodynamic shear zone is one of the most important mechanisms for the ductile and brittle failures in Earth, such as earthquakes [*Ogawa*, 1987; *Regenauer-Lieb and Yuen*, 2003; *John et al*., 2009], subduction initiation [*Regenauer-Lieb et al*., 2001], and slab detachment [*Gerya et al*., 2004]. The shear zone, which refers to the narrow zone of intensively localized plastic strain, occurs irreversibly, when materials with the strain energy exceeding the energy storage capability begin to release abruptly the stored strain energy as a form of heat or mechanical motion. Regarding the factors related to the development of shear zone, there have been various mechanisms discussed, such as crack propagation [*Andrews*, 2005], the inelastic interaction between granular grains [*Scott*, 1996; *Mora and Place*, 1998], flash heating [*Rice*, 2006], and the positive feedback between heat dissipation and strength softening [*Braeck and Podladchikov*, 2007]. Some theoretical works based on thermodynamics [e.g., *Lieou and Langer*, 2012] have contributed to derive the equation of state for the shear zone. Since the main focus of our study is on the effects of activation energy, which determines the degree of temperature dependence of rheology, we have paid attention to the thermally activated positive feedback (i.e., shear heating). The shear zone formation with shear heating in various materials has been extensively investigated to understand the transition from ductile to brittle regimes [e.g., *Lavier et al*., 2013] and the shear instability with bimaterial elastic heterogeneities [e.g., *So et al*., 2012]. However, the influence of activation energy on plastic flow for given environmental conditions, such as initial temperature and amount of deformation, has not been studied up to now. For more vigorous feedback accompanying the stronger heat dissipation, attempts were made to determine factors that decrease the activation energy, such as volatiles and water [e.g., *Karato and Jung*, 2003], because lower activation energy is thought to allow a higher plastic strain rate. However, the material with low activation energy may not support large stress. This means that low activation energy in a material does not guarantee strong shear heating. On the other hand, high activation energy can maintain high stress, which may cause strong heating even though the strain rate is small. Based on this mechanism, we may surmise that there can exist certain stationary points in activation energy for sustaining local minimum and maximum shear heating. To investigate this important issue, we perform a series of viscoelastoplastic thermal-mechanical calculations to determine the precise conditions for providing minimum and maximum dissipation for a given deformational setting.

2. Numerical Method

In this viscoelastoplastic two-dimensional numerical study, we adopt the finite element code, ABAQUS [*Hibbit, Karlsson, and Sorensen, Inc.*, 2009], to solve the conservation laws of mass, momentum, and energy with a power law rheology. To cover a wide range of rheological parameters, we perform a nondimensionalization using melting temperature, shear modulus, and thermal diffusivity as scaling factors [*Kaus and Podladchikov*, 2006]. In sections A1 and A2 of the supporting information, we derive mathematically the dimensionless forms of governing equations and power law rheology. Dimensionless continuity (equation (1)), momentum (equation (2)), and energy (equation (3)) equations for constant thermal diffusivity are given by

$$\frac{\partial \tilde{v}_i}{\partial \tilde{x}_i} = 0, \tag{1}$$

$$\frac{\partial \tilde{\sigma}_{ij}}{\partial \tilde{x}_j} = 0, \tag{2}$$

$$\frac{\partial \tilde{T}}{\partial \tilde{t}} + \tilde{v}_i \frac{\partial \tilde{T}}{\partial \tilde{x}_i} = \frac{\partial^2 \tilde{T}}{\partial \tilde{x}_j{}^2} + B\tilde{\tau}_{ij} : \tilde{\dot{\varepsilon}}_{ij}^{\mathrm{pl}} \quad \text{where} \quad B = \frac{\sigma_Y{}^2}{\rho c_P T_m G}. \tag{3}$$

~ denotes dimensionless quantities. σ_{ij} and τ_{ij} mean, respectively, the Cauchy and deviatoric stress tensor [e.g., *Karrech et al.*, 2011]. T, v, ρ, c_P, G, T_m, and σ_Y represent the temperature, velocity, density, specific heat, shear modulus, the melting temperature at ambient pressure, and the predefined plastic yield strength, respectively. The time and spatial coordinates are t and x. The meaning and values of all parameters are shown in Table S1 in the supporting information. Shear heating is a particular type of dissipative behavior, which exhibits the multiscale nature of time-dependent release of stored elastic strain energy when the shear zone appears after the medium has yielded plastically [*Landau and Lifshitz*, 1963]. Shear heating is mathematically approximated as $\tilde{\tau}_{ij} : \tilde{\dot{\varepsilon}}_{ij}^{\mathrm{pl}}$ and included in the equation of energy conservation (see equation (3)) [e.g., *So et al.*, 2013].

Dimensionless total strain rate tensor is simply defined by the sum of elastic and plastic strain rate tensors:

$$\tilde{\dot{\varepsilon}}_{ij}^{\mathrm{total}} = \tilde{\dot{\varepsilon}}_{ij}^{\mathrm{el}} + \tilde{\dot{\varepsilon}}_{ij}^{\mathrm{pl}} = \frac{1}{2}\frac{D\tilde{\tau}_{ij}}{D\tilde{t}} + \tilde{\dot{\varepsilon}}_{ij}^{\mathrm{pl}} \quad \text{where} \quad \frac{D\tilde{\tau}_{ij}}{D\tilde{t}} = \frac{\partial \tilde{\tau}_{ij}}{\partial \tilde{t}} + \tilde{v}_i \frac{\partial \tilde{\tau}_{ij}}{\partial \tilde{x}_i} - \tilde{W}_{ik}\tilde{\tau}_{kj} + \tilde{\tau}_{ik}\tilde{W}_{kj}. \tag{4}$$

$D/D\tilde{t}$ and $\tilde{W}_{ik}$ are, respectively, the objective Jaumann derivative and material spin rate tensor given by $\frac{1}{2}(\partial \tilde{v}_i/\partial \tilde{x}_k - \partial \tilde{v}_k/\partial \tilde{x}_i)$. When the material satisfies the von Mises yield function [*Hill*, 1950]

$$\tilde{J}_2 - 1 \geq 0 \ \text{ where } \ \tilde{J}_2 \ \text{ is the second invariant of } \ \tilde{\tau}_{ij} \ \text{ defined by } \ \sqrt{\frac{1}{2}\tilde{\tau}_{ij} : \tilde{\tau}_{ij}} \ , \tag{5}$$

$\tilde{\dot{\varepsilon}}_{ij}^{\mathrm{pl}}$ is activated and included into the calculation of equations (1)–(5). $\dot{\varepsilon}_{ij}^{\mathrm{pl}}$ shows power law stress and exponential temperature dependences as a creeping flow [e.g., *Karato and Spetzler*, 1990] written as

$$\tilde{\dot{\varepsilon}}_{ij}^{\mathrm{pl}} = D\tilde{J}_2^{n-1}\tilde{\tau}_{ij} \exp\left(-\mathrm{Ar}\frac{1}{\tilde{T}}\right) \quad \text{where} \quad \mathrm{Ar} = \frac{E_a}{RT_m} \quad \text{and} \quad D = \exp\left(\frac{E_R}{RT_m}\right). \tag{6}$$

E_R is a predefined reference activation energy of 500 kJ/mol. We calculate the dimensionless temperature of calculation domain with different Ar and amounts of deformation (%) with a fixed value of B, which means that material properties, except for E_a, are kept constant. We have used olivine $(\mathrm{Mg\text{-}Fe})_2\mathrm{SiO}_4$ for deriving values of B and Ar. Olivine is the most dominant component of the mantle and lithosphere of terrestrial planets [*Karato*, 2008]. According to experimental studies [e.g., *Durham and Goetze*, 1977], the representative B value of the olivine is $6.5 \cdot 10^{-4}$ (see Table S1). Although T_m can be altered by the confined pressure [e.g., *Davis and England*, 1964] and composition (i.e., Mg to Fe ratio) [*Roeder and Emslie*, 1970], those effects are negligible in our study. Thus, the value of D (i.e., the preexponential factor for the plastic creep) is constant in all models, and only temperature effect is important in determining the relation between deviatoric stress and plastic strain rate (see equation (6)).

We impose a defect with short wavelength in order to focus the strain [*Poirier*, 1980; *Regenauer-Lieb and Yuen*, 1998] (see Figure 1a). The domain has a dimensionless width L and height $1.7 \cdot 10^{-1}L$ with the square-shaped defect $10^{-2}L \times 10^{-2}L$ at the middle of the top boundary. The dimensionless initial temperature is uniformly distributed at $\tilde{T}_0 = T_0/T_m$. The fully coupled Jacobian matrix [*Zienkiewicz and Taylor*, 2000] derived based on equations (1)–(6) is numerically solved using the finite element method. Around the defect zone in which the

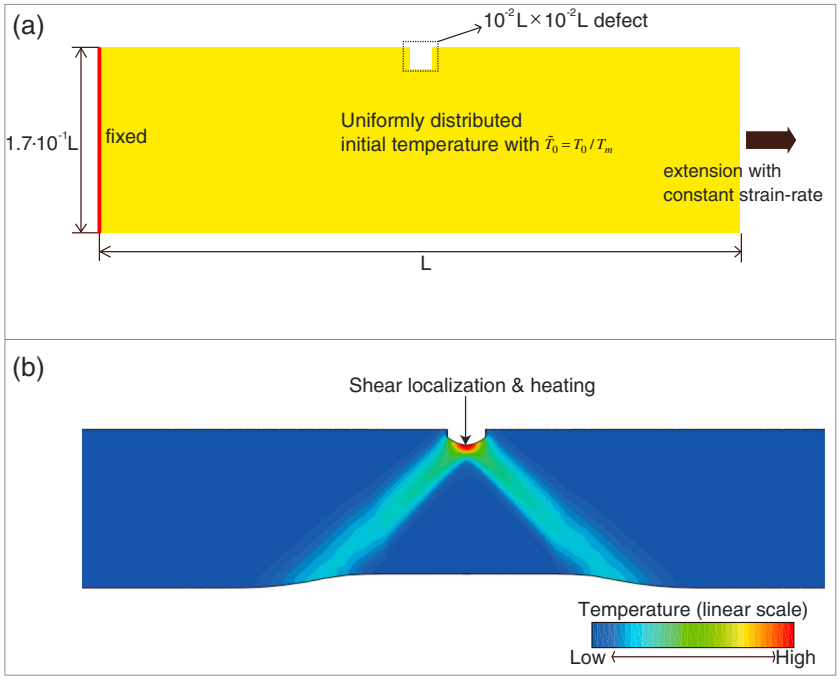

Figure 1. (a) Schematic description for our numerical model setup. The rectangular domain with aspect ratio of 1:6 is deformed with constant strain rate boundary condition. The left vertical boundary is fixed. All boundaries are thermally insulated. Thus, the feature of geodynamic shear zone is determined by the interplay between mechanical heat generation and heat conduction within the domain. (b) General feature of the shear zone formation in our study. The shear instability initiates at the defect. Then, the instability propagates toward the bottom boundary with 45° inclination. The color bar means the temperature. With different amounts of deformation and initial temperature, the temperature of the shear zone is different, but general features are similar.

instability is expected to occur, we defined Lagrangian quadratic type elements with grid size of $10^{-5}L$. Otherwise, the grid size far from the defect is relaxed to ~ $10^{-3}L$. The total number of nodes is ~10^7. Under this grid spacing, more than 200 elements exist across the shear zone, which means enough resolution to calculate shear heating. In addition, we performed the same calculations over finer and coarser grids to check for the convergence of solution in grid size. Detailed description of the time-integration method is stated in section A3 in the supporting information. The domain is deformed with constant strain rate of $10^{-13}\,s^{-1}$, which is geologically reasonable value for causing a strong shear heating [e.g., *Kelemen and Hirth*, 2007]. The domain is extended up to ~60% from an initial configuration. Since many extensional basins on the Earth show very large extension (i.e., > 60%) [e.g., *Chen*, 2014], a large amount of deformation should be considered in this study. Since all boundaries of domain are thermally insulated, the shear heating is generated under the near-adiabatic condition. With a small amount of deformation (i.e., ~2.8% extension), the shear instability initiates around the defect and propagates quickly toward the bottom (see Figure 1b). The instability reaches the bottom at ~3.1% deformation. We determine the average temperature, plastic strain rate, and stress at the defect with varying dimensionless Ar, $\widetilde{T}_0$, and duration of deformation.

3. Results and Discussion

We calculate the temperature elevation by shear heating with varying Ar and the amount of deformation in the case of $\widetilde{T}_0 = 0.25$ (see Figure 2). We can clearly recognize that the nonmonotonic variation of the temperature elevation with increasing Ar in each case with different amount of deformation. Two stationary points in Ar, Ar_{min}, and Ar_{max} can be discerned for the two stationary points for shear heating. The Ar difference between two stationary points, Ar_{max}-Ar_{min}, is generally ~15, which corresponds to ~200 kJ/mol. Between two stationary points Ar_{min} and Ar_{max}, the dimensionless temperature elevation increases with growing Ar values, which directly refers to the increasing E_a. This result is not consistent with the general consensus that materials with large activation energy do not exhibit strong shear heating due to the large

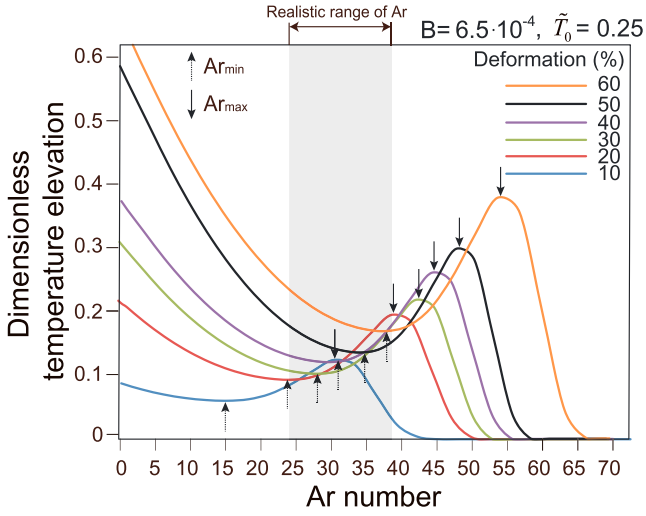

Figure 2. Dimensionless temperature elevation with varying dimensionless Ar. For calculating the dimensionless parameter B, we used $\rho = 3000$ kg/m^3, $c_P = 800$ J/kg·K, G = 8·10^{10} Pa, $T_m = 2000$ K, and $\sigma_Y = 500$ MPa (see equation (3) and Table S1). There are local minimum (at Ar = Ar$_{min}$, see dashed arrows) and maximum (at Ar = Ar$_{max}$, see solid arrows) of temperature elevation in each cases of different amounts of deformation. The retrogression, which the shear heating is stronger in larger Ar (i.e., larger E_a), is shown in cases that Ar value is between Ar$_{min}$ and Ar$_{max}$. The shaded zone refers the Ar range based on laboratory experiments. The temperature elevation of the case of 30% deformation seems to be great in the shaded zone.

energy barrier against plastic deformation. For the case of a small amount extension (i.e., 10%, see the blue line in Figure 2), the Ar$_{max}$ exists within the realistic range of Ar (see the shaded zone in Figure 2), while the Ar$_{min}$ lies out of the range. When the Ar is Ar$_{max}$ (i.e., = 32), the shear heating is locally maximum. Therefore, we may deduce that the shear zone can effectively act as a weak zone. Otherwise, at the point of Ar = 37, the shear heating is weaker by a factor of ~10. The Ar difference of 5 corresponds to only 65 kJ/mol (in activation energy), which can easily appear in geological situation such as water content variation. It has an important implication for geological deformation associated with shear heating such as finite amplitude folding and frictional sliding. If the deforming domains have slightly different Ar number compared with Ar$_{max}$, there is no or very weak shear heating. The deformation with shear heating is significantly sensitive in the Ar number. This means that precise measurement of activation energy and its variation with volatiles should be fully determined. For the case of 20% deformation (see the red curve in Figure 2), it is completely counterintuitive situation within the realistic range of Ar. The larger activation energy is assigned; the larger shear heating is generated. According to our research, we found that people need to consider this counterintuitive phenomenon in analyzing geological deformation. In the case of 60% deformation (see the orange curve), it is a rather intuitive situation within the realistic range. We may argue that lowering the activation energy can enhance the shear heating and the subsequent dynamics deformation when the background deformation is large (i.e., >60%). This trend suggests that the activation energy for the minimum and maximum heat dissipation could be dynamically changed with deformation history. This finding should force greater attention on the relationship between activation energy and the amount of deformation in predicting when the geological structure would fail or would still remain intact.

The amount of shear heating is determined by the contraction between the deviatoric stress $\tilde{\tau}_{ij}$ and the plastic strain rate $\dot{\tilde{\varepsilon}}^{pl}_{ij}$ tensors (see the last term in equation (1)). To investigate the cause of the variations in heat production as a function of Ar, the strain rate and stress should be considered separately and quantified. For this reason, we define two dimensionless quantities related with $\dot{\tilde{\varepsilon}}^{pl}_{ij}$ and $\tilde{\tau}_{ij}$. The first is the dimensionless equivalent plastic strain rate $\dot{\tilde{\varepsilon}}^{pl}_{eq} = \sqrt{\frac{2}{3}\dot{\tilde{\varepsilon}}^{pl}_{ij} : \dot{\tilde{\varepsilon}}^{pl}_{ij}}$ (see Figure 3a), while the other is the dimensionless von Mises deviatoric stress $\tilde{\tau}_v = \sqrt{\frac{3}{2}\tilde{\tau}_{ij} : \tilde{\tau}_{ij}}$ (see Figure 3b). In every time step, we calculate the $\dot{\tilde{\varepsilon}}^{pl}_{eq}$ and $\tilde{\tau}_v$, which give measures of $\dot{\tilde{\varepsilon}}^{pl}_{ij}$ and $\tilde{\tau}_{ij}$, respectively. In Figure 3a, we plot the relationship between the dimensionless equivalent plastic strain rate $\dot{\tilde{\varepsilon}}^{pl}_{eq}$ and the deformation ratio (%) with varying Ar. For Ar < Ar$_{min}$, very large plastic strain rate appears quickly as soon as the deformation begins because the material is too deformable due to the small E_a. The $\dot{\tilde{\varepsilon}}^{pl}_{eq}$ in steady state is smaller for a larger Ar (compare black and red dotted lines in Figure 3a). In contrast, the $\dot{\tilde{\varepsilon}}^{pl}_{eq}$ increases with increasing Ar when Ar$_{min}$ ≤ Ar ≤ Ar$_{max}$. This opposite trend between $\dot{\tilde{\varepsilon}}^{pl}_{eq}$ and Ar indicates that more efficient thermal strain feedback occurs regardless of increasing E_a, if

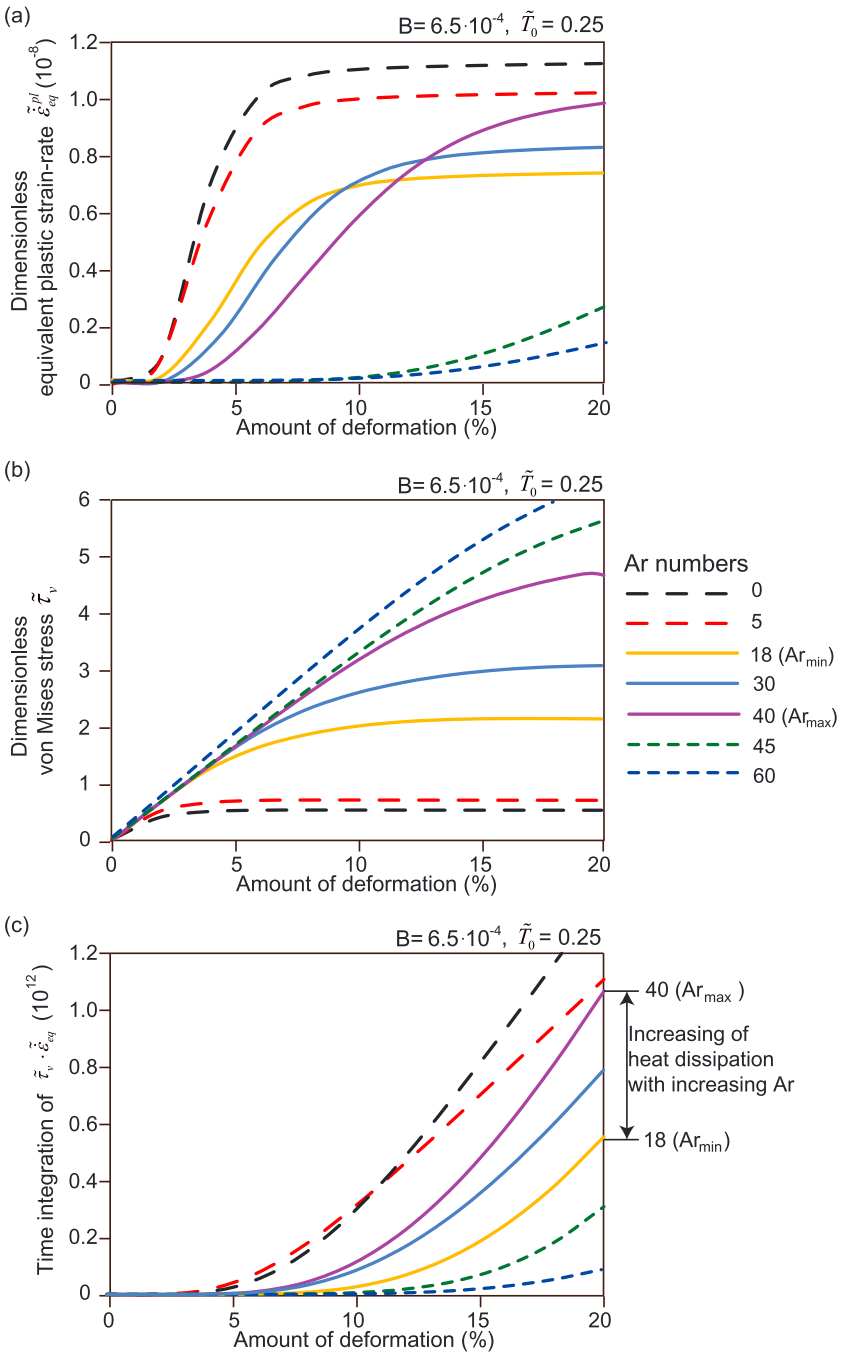

Figure 3. (a) The variation of dimensionless plastic strain rate with different Ar numbers. Generally, smaller Ar (i.e., smaller activation energy) shows larger strain rate following power law nature of rheology. However, between Ar_{min} and Ar_{max}, the retrogression appears. (b) The variation of deviatoric stress with different Ar. The models with larger Ar can support larger stress. (c) The total amount of shear heating during the deformation. Considering the case of $Ar < Ar_{min}$, the plastic strain rate is very high, while the stress is very low. Consequently, the shear instability is strong enough to heat up the defect of domain. The multiplication of strain rate and deviatoric stress at $Ar = Ar_{max}$ is optimal.

the condition of Ar is between Ar_{min} and Ar_{max}. For values above Ar_{max}, the $\tilde{\dot{\varepsilon}}^{pl}_{eq}$ values are very small, and steady state is not achieved within the deformation time. The stress regime with different Ar also needs to be determined. In Figures 3b, the von Mises deviatoric stress $\tilde{\tau}_v$ is plotted with different amounts of deformation and Ar numbers. Even though the elements of $\tilde{\sigma}_v$ exceed the predefined yield strength $\tilde{\sigma}_Y = 1$,

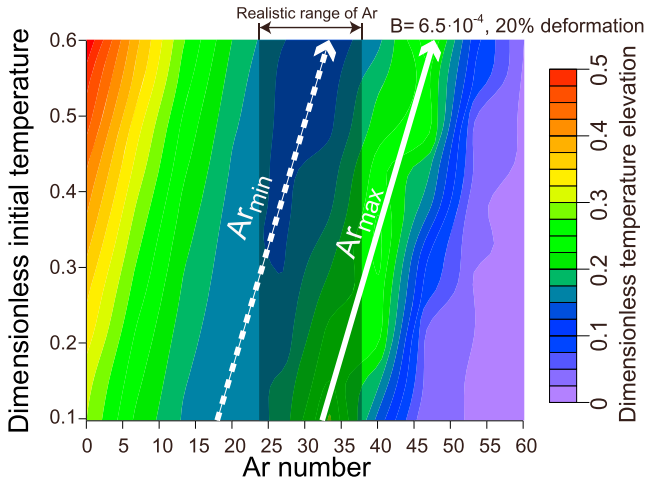

Figure 4. Dimensionless temperature elevation at 20% deformation for varying dimensionless $\widetilde{T}_0$ values as well as Ar. Since the weaker strength (right after the plastic yielding) in the case of higher $\widetilde{T}_0$ cannot support large stress, the higher $\widetilde{T}_0$ case requires the larger Ar_{max}.

the elements do not immediately exhibit strain-softening behavior, but rather, the strain hardening is shown for a certain duration because of the energy barrier (i.e., E_a) against the initiation of plastic creeping.

Then, we calculate and display the integrated heat release over time $\int \widetilde{\tau}_v \cdot \widetilde{\dot{\varepsilon}}_{eq} d\widetilde{t}$ in Figure 3c for the case of $\widetilde{T}_0 = 0.25$ and 20% deformation. Results from Figure 3c are seen to be consistent with the trend in Figure 2. Both strain hardening and softening during the deformation of the model with $Ar < Ar_{min}$ (i.e., the cases of $Ar = 0$ and 5) are very small. However, because a large plastic strain rate compensates for the developed weak stress, shear heating can be vigorous. Although this condition seems to be suitable for fast material failure, these small values of Ar are unrealistic, based upon the rheology of various materials such as rocks and metals. $Ar = 0$ and 5 are corresponding to $E_a = 0$ and ~62 kJ/mol, respectively. In the case of $Ar > Ar_{max}$, the state of strain rate and stress is opposite to that of the case of $Ar < Ar_{min}$. In the case of $Ar = 60$, the applied stress is large. However, this larger stress apparently does not compensate for the small plastic strain rate. The amount of heat dissipation is consequently small. At $Ar = Ar_{min}$, both the stress and the strain rate are small. This situation causes the local minimum shear heating (see the orange line in Figure 3). In the case of $Ar = Ar_{max}$ (see the purple line in Figure 3), the values of $\int \widetilde{\tau}_v \cdot \widetilde{\dot{\varepsilon}}_{eq} d\widetilde{t}$ is the local maximum because of sufficiently large strain rate and deviatoric stress, and the subsequent strong energy dissipation cooperatively induces the maximum shear heating. We may propose the existence of two values of Ar for the local stationary points of shear heating. Although present paper did not include multigrain system, some laboratory experimental studies have reported that the heterogeneous distribution of strain weakening during the dynamic grain size evolution causes the shear instability [*Hansen et al.*, 2012]. In addition, some theoretical studies have proposed the important connection between grain size and mechanical work under a two-phase environment [*Bercovici and Ricard*, 2012].

The 2-D contour plot in Figure 4 shows the increase in temperature by shear heating versus the initial temperature $\widetilde{T}_0$ and Ar at a deformation of 20%. Similarly with Figure 2, we find that there exist clear stationary points Ar_{min} (see the dashed arrow in Figure 4) and Ar_{max} (see the solid arrow in Figure 4) corresponding to the local minimum and maximum of temperature rise, respectively. The realistic Ar values based on experimentally derived E_a (see the shaded zone in Figure 4) are between 24 (i.e., ~300 kJ/mol of wet olivine) and 37.30 (i.e., ~465 kJ/mol of dry olivine) [*Evans and Kohlstedt*, 1995]. We can recognize clearly that the predefined values of $\widetilde{T}_0$ determine the location of the stationary points Ar_{min} and Ar_{max} within the shaded region. In cases of $\widetilde{T}_0 < 0.3$, neither Ar_{min} nor Ar_{max} lies in the shaded zone, indicating that the larger E_a overcomes the nonlinearity and subsequent heat dissipation. For cases of $\widetilde{T}_0 > 0.3$, at least one stationary point exists in the shaded zone. In these cases, the E_a influences the amount of heat dissipation in a nonmonotonic manner where increasing of E_a causes both increasing and decreasing of the shear heating. The case of the higher $\widetilde{T}_0$ exhibits a larger Ar_{min} and Ar_{max}. Otherwise, under the environment of low $\widetilde{T}_0$, the low E_a can create the local maximum shear heating. In the two contrary cases of $\widetilde{T}_0 = 0.1$ and 0.4, the values of Ar_{max} are 30 and 45, respectively. Because the strength of the material with high $\widetilde{T}_0$ is weak right after the plastic yielding occurs, the material with a higher $\widetilde{T}_0$ value requires a long duration of deformation, which is regarded as the duration of strain-energy accumulation. This behavior has an important implication for the ductile creep and shear localization leading to the ultimate failure. In particular, the shear zone in the

Earth can appear under both low- (i.e., near-surface) and high-temperature (i.e., deep interior) environments. In the near-surface, the most puzzling phenomena related with shear heating are subduction initiation, which refer to the situation where an oceanic plate begins to underthrust the continental plate [*Stern*, 2004]. Since this instability is formed in a low-temperature condition, reducing E_a by water [e.g., *Regenauer-Lieb et al*., 2001] can enhance the destabilization. In contrast, the deep interior of terrestrial planets is very hot because of collisional heating during the formation of the protoplanet and radioactive heating [*Safronov*, 1978]. Adiabatic shear heating and subsequent rock melting [*Orowan*, 1960] have been suggested as mechanisms of deep focus earthquake. For high-temperature conditions, the E_a for maximum shear heating can be large and thus enable sufficient strain-energy accumulation and vigorous heat dissipation. Moreover, this study is relevant for the problem dealing with the creep of amorphous rock near the glass transition temperature [*Meade and Jeanloz*, 1987].

We applied the elasticity (see equations (3) and (4)) in modeling of shear zone formation. In long timescale geodynamics such as a ductile shear zone development, the elasticity has been relatively ignored compared with viscous behavior, because people have thought that the elasticity covers only the short timescale phenomena. However, recent numerical studies revealed that the elasticity determines the amount of elastic energy storage in early stage of deformation, then can dominantly control the long-term geodynamical process [e.g., *Regenauer-Lieb et al*., 2012]. We have proposed that the elasticity should be considered in handling of long timescale geodynamical problems.

4. Concluding Remarks

We report here that stationary values of E_a exist for the local maximum and minimum of shear heating for a given amount of deformation and initial temperature. When we assign a larger amount of deformation and/or higher initial temperature, the required E_a for the maximum shear heating also becomes higher. The power law relationship between $\dot{\varepsilon}_{ij}^{\mathrm{pl}}$ and τ_{ij} is linked tightly to the deformation history and the background thermal structure. This finding does have important bearing for geodynamics, because of these connections. A larger E_a guarantees a greater strength of the material, yet it cannot allow a larger $\dot{\varepsilon}_{ij}^{\mathrm{pl}}$. On the other hand, a smaller E_a allows the material to creep easier, but the applied stress is weak. This trade-off effect between $\dot{\varepsilon}_{ij}^{\mathrm{pl}}$ and τ_{ij} induces stationary points in activation energy for local maximum and minimum of heat dissipation. Since the development of geodynamic shear zone is an important mechanism for the plastic failure, which can occur over a wide range of initial temperature and spatial scales, our research for the stationary E_a in a given condition provides vital information on evaluating the possibility of the formation of a shear zone in lithospheric dynamics. The difference in the two stationary E_a values of $\mathrm{Ar}_{\mathrm{max}}$ and $\mathrm{Ar}_{\mathrm{min}}$ is generally ~200 kJ/mol for olivine mineral. However, the E_a difference of two stationary points could be much smaller in different material with different and more complicated rheology (e.g., the power law exponent, n), which means that the role of heat dissipation in lithospheric dynamics with deformational history and initial temperature can be much more sensitive than olivine. Moreover, the size ratio between the entire domain and the defect may influence the existence of stationary points. The size of defect can span from nanometers to thousands of kilometers. Therefore, further investigation should be performed with various materials and sizes of defect and domain, because this may shed light on the multiscale features observed in plate tectonics.

Acknowledgments

We thank Stefan Schmalholz and Masanori Kameyama for their constructive reviews to improve this work. We thank Sandy Cruden and Fabio Capitanio from Monash University and Yuri Podladchikov from University of Lausanne for useful discussions. This grant was supported in part by Geochemistry and CMG programs of U.S. National Science Foundation and by Korean government (MEST, 2009-0092790).

The Editor thanks Stephan Schmalholz and Masanori Kameyama for their assistance in evaluating this paper.

References

Andrews, D. J. (2005), Rupture dynamics with energy loss outside the slip zone, *J. Geophys. Res.*, *110*, B01307, doi:10.1029/2004JB003191.

Bercovici, D., and Y. Ricard (2012), Mechanisms for the generation of plate tectonics by two-phase grain-damage and pinning, *Phys. Earth Planet. Int.*, *202–203*, 27–55.

Braeck, S., and Y. Y. Podladchikov (2007), Spontaneous thermal runaway as an ultimate failure mechanism of materials, *Phys. Rev. Lett.*, *98*, 095504, doi:10.1103/PhysRevLett.98.095504.

Chen, L. (2014), Stretching factor estimation for the long-duration and multi-stage continental extensional tectonics: Application to the Baiyun Sag in the northern margin of the South China Sea, *Tectonophysics*, *611*, 167–180.

Davis, B. T. C., and J. L. England (1964), The melting of forsterite up to 50 kbars, *J. Geophys. Res.*, *69*(6), 1113–1116, doi:10.1029/JZ069i006p01113.

Durham, W. B., and C. Goetze (1977), Plastic flow of oriented single crystals of olivine: 1. Mechanical data, *J. Geophys. Res.*, *82*(36), 5737–5753, doi:10.1029/JB082i036p05737.

Evans, B., and D. Kohlstedt (1995), *Rock Physics and Phase Relations: A Handbook of Physical Constants (AGU Reference Shelf 3)*, AGU, Washington, D. C.

Gerya, T. V., D. A. Yuen, and W. V. Maresch (2004), Thermomechanical modelling of slab detachment, *Earth Planet. Sci. Lett.*, *226*(1–2), 101–116.

Hansen, L. N., M. E. Zimmerman, A. M. Dillman, and D. L. Kohlstedt (2012), Strain localization in olivine aggregates at high temperature: A laboratory comparison of constant-strain-rate and constant-stress boundary conditions, *Earth Planet. Sci. Lett.*, *333–334*, 134–145, doi:10.1016/j.epsl.2006.03.029.

Hibbit, Karlsson, and Sorensen, Inc. (2009), ABAQUS user's manual version 6.9, vol. 1, Pawtucket, R. I.

Hill, R. (1950), *The Mathematical Theory of Plasticity*, Oxford Univ. Press, New York.

John, T., S. Medvedev, L. H. Rüpke, T. B. Andersen, Y. Y. Podladchikov, and H. Austrheim (2009), Generation of intermediate-depth earthquakes by self-localizing thermal runaway, *Nat. Geosci.*, *2*, 137–140, doi:10.1038/ngeo419.

Karato, S. (2008), *Deformation of Earth Materials: An Introduction to the Rheology of Solid Earth*, Cambridge Univ. Press, London, U. K.

Karato, S., and H. Jung (2003), Effects of pressure on high-temperature dislocation creep in olivine polycrystals, *Philos. Mag.*, *83*, 401–414.

Karato, S., and H. A. Spetzler (1990), Defect microdynamics in minerals and solid-state mechanisms of seismic wave attenuation and velocity dispersion in the mantle, *Rev. Geophys.*, *28*(4), 399–421, doi:10.1029/RG028i004p00399.

Karrech, A., K. Regenauer-Lieb, and T. Poulet (2011), Continuum damage mechanics for the lithosphere, *J. Geophys. Res.*, *116*, B04205, doi:10.1029/2010JB007501.

Kaus, B. J. P., and Y. Y. Podladchikov (2006), Initiation of localized shear zones in viscoelastoplastic rocks, *J. Geophys. Res.*, *111*, B04412, doi:10.1029/2005JB003652.

Kelemen, P. B., and G. Hirth (2007), A periodic shear-heating mechanism for intermediate-depth earthquakes in the mantle, *Nature*, *446*, 787–790, doi:10.1038/nature05717.

Landau, L. D., and E. M. Lifshitz (1963), *Fluid Mechanics*, Pergamon Press, Oxford, U. K.

Lavier, L. L., R. A. Bennett, and R. Duddu (2013), Creep events at the brittle ductile transition, *Geochem. Geophys. Geosyst.*, *14*, 3334–3351, doi:10.1002/ggge.20178.

Lieou, C. K. C., and J. S. Langer (2012), Nonequilibrium thermodynamics in sheared hard-sphere materials, *Phys. Rev. E*, *85*, 061308, doi:10.1103/PhysRevE.85.061308.

Meade, C., and R. Jeanloz (1987), Frequency-dependent equation of state of fused silica to 10 GPa, *Phys. Rev. B*, *35*(1), 236–242.

Mora, P., and D. Place (1998), Numerical simulation of earthquake faults with gouge: Toward a comprehensive explanation for the heat flow paradox, *J. Geophys. Res.*, *103*(B9), 21,067–21,089, doi:10.1029/98JB01490.

Ogawa, M. (1987), Shear instability in a viscoelastic material as the cause of deep focus earthquakes, *J. Geophys. Res.*, *92*, 13,801–13,810, doi:10.1029/JB092iB13p13801.

Orowan, E. (1960), Mechanism of seismic faulting, *Geol. Soc. Am. Mem.*, *79*, 323–345.

Poirier, J.-P. (1980), Shear localization and shear instability in materials in the ductile field, *J. Struct. Geol.*, *2*(1–2), 135–142, doi:10.1016/0191-8141(80)90043-7.

Regenauer-Lieb, K., and D. A. Yuen (1998), Rapid conversion of elastic energy into plastic shear heating during incipient necking of the lithosphere, *Geophys. Res. Lett.*, *25*, 2737–2740, doi:10.1029/98GL02056.

Regenauer-Lieb, K., and D. A. Yuen (2003), Modelling shear zones in geological and planetary sciences: Solid- and fluid-thermal-mechanical approaches, *Earth Sci. Rev.*, *63*, 295–349.

Regenauer-Lieb, K., D. A. Yuen, and J. M. Branlund (2001), The initiation of subduction: Criticality by addition of water?, *Science*, *294*(5542), 578–580.

Regenauer-Lieb, K., R. F. Weinberg, and G. Rosenbaum (2012), The role of elastic stored energy in controlling the long term rheological behaviour of the lithosphere, *J. Geodyn.*, *55*, 66–75.

Rice, J. R. (2006), Heating and weakening of faults during earthquake slip, *J. Geophys. Res.*, *111*, B05311, doi:10.1029/2005JB004006.

Roeder, P. L., and R. F. Emslie (1970), Olivine-liquid equilibrium, *Contrib. Mineral. Petrol.*, *29*, 275–289, doi:10.1007/BF00371276.

Safronov, V. S. (1978), The heating of the earth during its formation, *Icarus*, *33*, 3–12.

Scott, D. R. (1996), Seismicity and stress rotation in a granular model of the brittle crust, *Nature*, *381*, 592–595.

So, B.-D., D. A. Yuen, K. Regenauer-Lieb, and S.-M. Lee (2012), Asymmetric lithospheric instability facilitated by shear modulus contrast: Implications for shear zones, *Geophys. J. Int.*, *190*(1), 23–36, doi:10.1111/j.1365-246X.2012.05473.x.

So, B.-D., D. A. Yuen, and S.-M. Lee (2013), An efficient implicit-explicit adaptive time stepping scheme for multiple-time scale problems in shear zone development, *Geochem. Geophys. Geosyst.*, *14*, 3462–3478, doi:10.1002/ggge.20216.

Stern, R. J. (2004), Subduction initiation: Spontaneous and induced, *Earth Planet. Sci. Lett.*, *226*(3), 275–292.

Zienkiewicz, C., and R. L. Taylor (2000), *The Finite Element Method: The Basis*, vol. 1, 5th ed., Butterworth-Heinemann, Oxford, U. K.